Natural Resources Canada   Ressources naturelles Canada

GEOLOGICAL SURVEY OF CANADA
OPEN FILE 7711

Whole-rock lithogeochemistry and pXRF data from the Meliadine gold district, Nunavut, Canada

C.J.M. Lawley, B. Dubé, P. Mercier-Langevin, B.A. Kjarsgaard, and R.D. Knight

2015

Canada

GEOLOGICAL SURVEY OF CANADA
OPEN FILE 7711

Whole-rock lithogeochemistry and pXRF data from the Meliadine gold district, Nunavut, Canada

C.J.M. Lawley[1], B. Dubé[2], P. Mercier-Langevin[2], B.A. Kjarsgaard[1], and R.D. Knight[1]

[1]Natural Resources Canada, Geological Survey of Canada, 601 Booth Street, Ottawa, Ontario
[2]Natural Resources Canada, Geological Survey of Canada, 490, rue de la Couronne, Québec, Quebec

2015

doi:10.4095/296223

This publication is available for free download through GEOSCAN (http://geoscan.nrcan.gc.ca/).

Recommended citation
Lawley, C.J.M., Dubé, B., Mercier-Langevin, P., Kjarsgaard, B.A., and Knight, R.D., 2015. Whole-rock lithogeochemistry and pXRF data from the Meliadine gold district, Nunavut, Canada; Geological Survey of Canada, Open File 7711, 1 .zip file. doi:10.4095/296223

Publications in this series have not been edited; they are released as submitted by the author.

Introduction

This open file presents whole-rock lithogeochemical and portable X-Ray Fluorescence spectrometry (pXRF) data from the Meliadine gold district (MGD), Nunavut, Canada. The study was completed under the auspices of the Targeted Geoscience Initiative (TGI)-4 program in an effort to define and map the hydrothermal footprint at the MGD. Samples were collected from exploration drill core and outcrop along the newly constructed all-season road that links Rankin Inlet with the Meliadine Exploration camp (Fig. 1). Detailed ore deposit geology and lithogeochemical data presentation/interpretations are provided in Lawley et al. (in press). The sampling strategy and analytical methodology are described below.

Geology

The MGD is situated in what was originally defined as the Rankin Inlet Group (Bannatyne, 1958) and later referred to as the Rankin greenstone belt (e.g., Aspler and Chiarenzelli, 1996). Here, Neoarchean (ca. 2.66 Ga; Tella et al., 1996) mafic volcanic rocks (basalt dominated) are intercalated with mafic-intermediate-felsic volcaniclastic and interflow siliciclastic sequences, and Algoma-type Banded Iron Formation (BIF; Fig. 1). For the purposes of the current study, the MGD stratigraphy was simplified into three lithofacies: (1) turbidite (greywacke-siltstone-mudstone); (2) BIF (BIF-chert-argillite); and (3) volcanic (mafic volcanic rocks of basaltic-andesitic composition and associated interflow mafic volcaniclastic rocks). This simplified subdivision is based, in part, on geochemical similarities and the spatial relationship between lithologies that define each lithofacies (Lawley et al. in press).

The MGD is host to a number of significant orogenic greenstone- and BIF-hosted gold deposits: Tiriganiaq; Normeg; Wesmeg; F Zone, Pump, Wolf (not discussed) and Discovery (Fig. 1). Each gold deposit is situated proximal to, but north of, the E-W to WNW-ESE trending and steeply north-dipping Pyke Fault (Miller et al., 1995; Fig. 1). This fault and its associated splays, coupled with prominent Z-fold patterns, deform BIF and represent first-order controls on the distribution of gold (see Carpenter, 2003; Carpenter and Duke 2004; Carpenter et al., 2005 for further details).

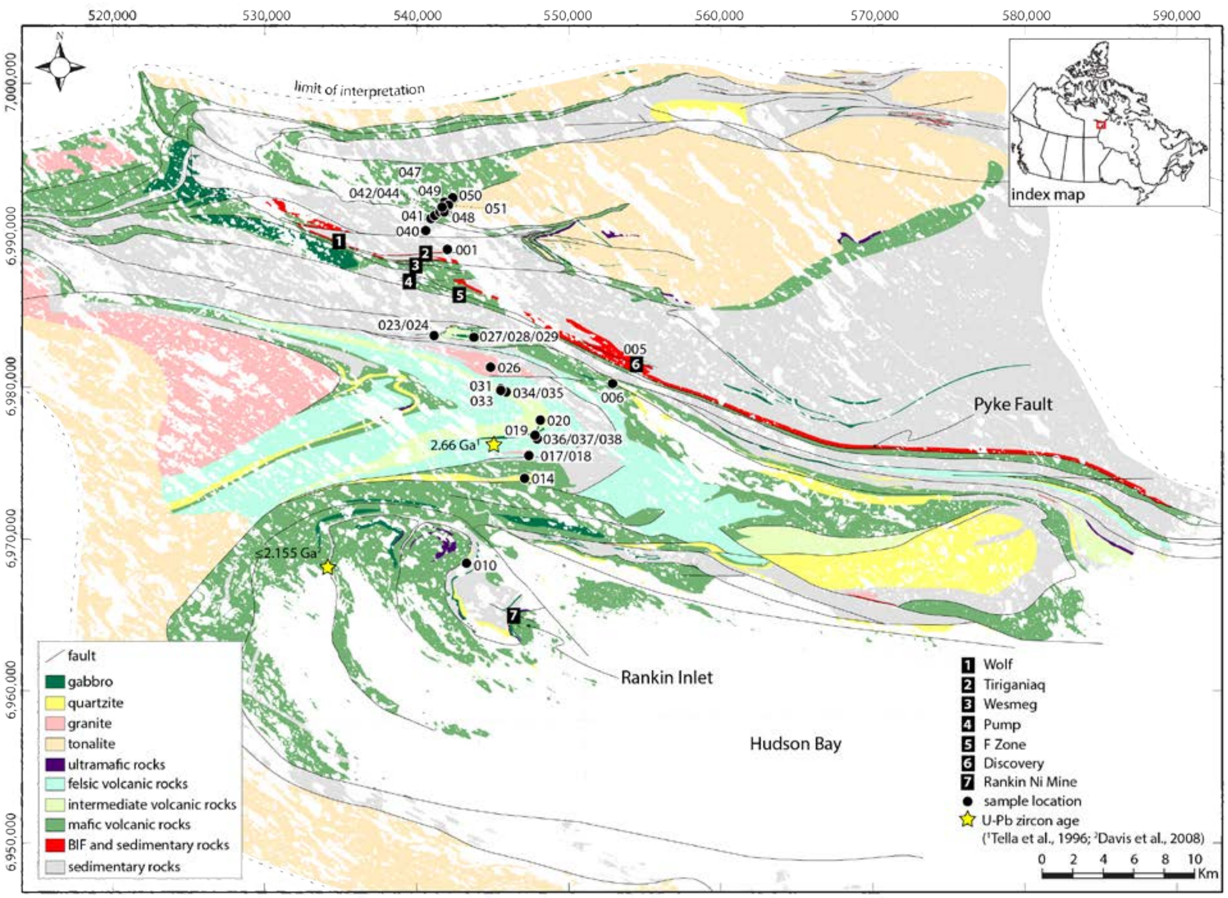

Figure 1 – Local geological map of the Meliadine gold district (map courtesy of Agnico-Eagle Mines Ltd.). The largest of the known gold deposits occur along the Pyke Fault (Wolf, Tiriganiaq, Wesmeg, Pump, F Zone, and Discovery). Regional geochemistry samples reported in the appended Table 1and the former Rankin Nickel Mine are shown for reference (UTM zone 15N, NAD83).

Sampling strategy

The data presented here come from eight exploration diamond drill holes that were selected for detailed sampling from six gold deposits, or ore zones, within the larger MGD gold-bearing hydrothermal system. Each of the selected holes was intended to represent a single transect from the non-mineralized hanging wall, through the ore zone and extending into the non-mineralized footwall based on Agnico Eagle Mines gold assay data (Fig. 2). Representative samples (typically 15 cm long split NQ-drill cores depending, in part, on grain size and sample homogeneity; veins were avoided where possible) were collected for each lithology and representative intervals of each mineral alteration assemblage and gross alteration intensity (e.g., least altered versus altered versus extremely altered). This approach resulted in a sampling density of approximately one sample per 3−6 m for each of the eight drill holes (M12-1877 had a lower average sampling density of one sample per ca. 10 m), although sampling density was typically much higher in the ore zones.

The F Zone deposit was selected for higher density-sampling (whole-rock and pXRF) due to its relatively simple stratigraphy of volcanic rocks interbedded with BIF. Three holes from a drill fan at the F Zone were selected in order to define the deposit's hydrothermal footprint in section. Whole-rock lithogeochemical sampling was completed every 3 m; whereas pXRF analyses were completed at least every 1.5 m for each of three F Zone exploration drill holes. In addition to the detailed exploration drill core sampling described above, a smaller subset of samples (n = 32) was collected from the regional Rankin Inlet stratigraphy (Fig. 1).

Whole-rock lithogeochemistry

All whole-rock geochemical analyses were completed at Actlabs in Ancaster, Ontario. Whole-rock drill core samples were initially pulverized in a chromium-free steel mill before agate milling until 85% of the sample material passed through a 75 μm mesh. Major and minor elements were analyzed via ICP-AES using a lithium meta-borate fusion. Trace element analyses were conducted using a combination of lithium meta-borate fusion ICP-AES and ICP-MS, aqua-regia ICP-MS and four-acid digestion ICP-MS for chalcophile elements. High-grade ore zone samples were re-analyzed with a combination of fire assay and gravimetric methods depending on the analyte. The analytical method with the lowest reported detection limits were used for data exploration and interpretation, with the fire assay and gravimetric methods results used for high-grade samples (Lawley et al., in press).

Quality control materials (standards and duplicates) were inserted by Actlabs for every 20 unknowns. In addition to these laboratory quality control measures, blind standards (Diorite Gneiss, SY-4, n = 12; Cu-ore, OREAS-111, n = 3; and Au-ore, DS-1, n= 2) and duplicates (n = 10) were submitted to the laboratory over the course of the project in order to act as an independent check on analytical precision and accuracy. Blind standards (n = 17) and duplicates (n = 10) are reported in the appended Table 1 (N.B. concentrations below the analytical detection limit are demarcated by a '<' symbol; whereas blank cells represent undetected analytes). Data are published as received from Actlabs.

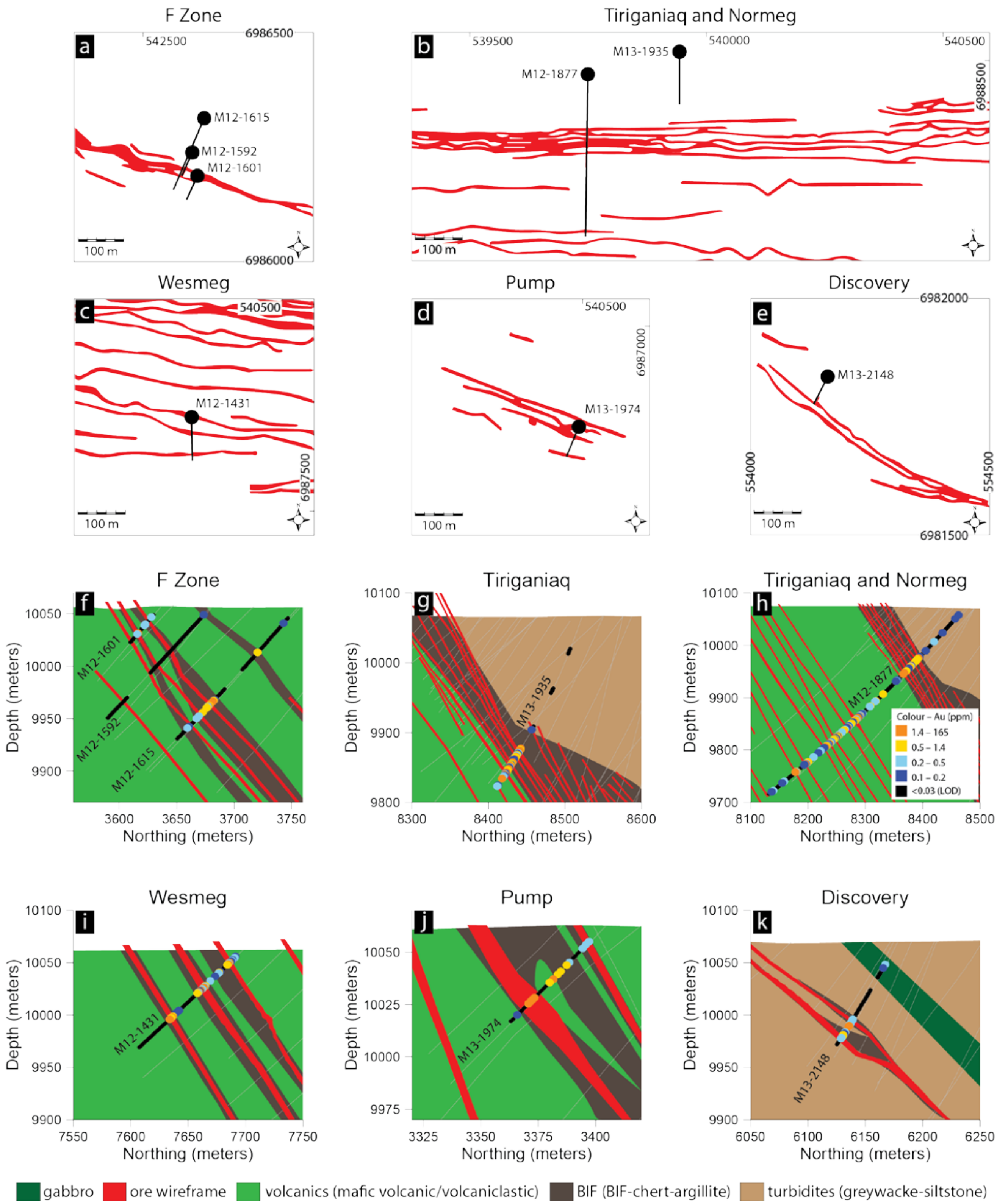

Figure 2 – Simplified plan views (a–e) and geologic sections (f–k) at each of the studied deposits. Plan views show the borehole traces and BIF-hosted gold ore zone wireframes projected to surface. Sections show the simplified geology and ore wireframes from 3D modelling at each deposit. Agnico-Eagle Mines Ltd. gold fire assays, divided into quartiles, are plotted alongside the trace of each of borehole.

pXRF

All pXRF analyses were acquired using a Thermo Scientific Niton XL3t GOLDD portable XRF spectrometer (serial number 37005) on the surface of cut exploration diamond drill core. The spectrometer is equipped with a Cygnet 50 kV, 2 watt, Ag Anode X-ray tube and a XL3 silicon drift detector and was mounted in a Thermo Scientific mobile test stand at the Agnico Eagle Mines Meliadine exploration camp. Analyses were repeated in 'soil' (optimized for element concentrations <1 wt. %, i.e., minor and trace elements) and 'mining' (optimized for concentrations >1 wt. %, i.e., major elements) modes for each sample spot using a 60 s dwell times for each of the Main, Low and High filters (total analysis time = 180 s; see Knight et al., 2013 for further analytical details).

Data acquisition followed a standard-sample-standard bracketing approach. A suite of four powdered certified reference materials (basalt, BIR-1; shale, Cody Shale; diabase, TDB-1; and Au-ore, DS-1) were analyzed after approximately 10−15 unknowns and were used as a means of quality control during each analytical session. Powdered reference materials were also used to calibrate pXRF analyses in order to compare pXRF results with conventional whole-rock lithogeochemistry for the same samples. However, this standard-sample-standard bracketing approach does not take into account variability (e.g., grain size) between the powdered reference materials and the analyzed rock surfaces.

We tested the validity of our calibration by preparing in-house rock reference pucks (i.e., rock slab slightly larger than the 1.5 cm pXRF analysis window). These in-house reference materials were matrix-matched to MGD rocks and possess a known composition based on replicate analyses via conventional whole-rock lithogeochemistry. The in-house reference material ('Wesmeg') was analyzed for each standard-sample-standard bracket and the results of these analyses are reported alongside powdered reference materials and sample analyses in the appended Table 2 (N.B. concentrations below detection limit are reported as blank cells; analytical uncertainties are reported at two standard deviations). A silica blank was analyzed at the start of each sample-standard bracket in order to monitor instrument background and the cleanliness of the pXRF analysis window and test stand. The precision (represented by % relative standard deviation; %RSD) and accuracy (measured as the % difference between average concentration and its accepted value; % DIF) of pXRF results, based on the quality control measures described above, are summarized in the appended Table 2.

Colorimetry

Quantitative colour measurements have not found wide spread use in the earth sciences; however hand-held colorimeters have become increasingly robust and offer colour detection that, under certain conditions, is more reliable than the human eye. For the purposes of this study, a handheld Eoptis CLM-94 colorimeter was used to acquire quantitative colour measurements (reported in CIELAB colour space) of dry rock diamond drill core surfaces over approximately the same spot as each pXRF analysis (the 20 mm diameter colorimeter analysis window is larger than the 8 mm pXRF analysis window). Although not specifically designed for rock analysis, the Eoptis colorimeter uses circumferential illumination and a measurement geometry (45°C:0°) that makes it ideally suited for textures surfaces (like that of a rock surface). However caution must be emphasized when comparing results between rock types since results are dependent on a number of factors including: (1) grain size; (2) mineralogy; (3) sample opacity/translucency; (4) sample homogeneity; and (5) analytical conditions (moisture, temperature, etc.). Colour calibration and quality control was completed using a reference patch provided by Eoptis and analyzed after approximately 20 unknowns. An example of the application of colorimeter is presented in a heat map (Figure 3), which shows colour measurements in LAB-space plotted alongside pXRF analyses.

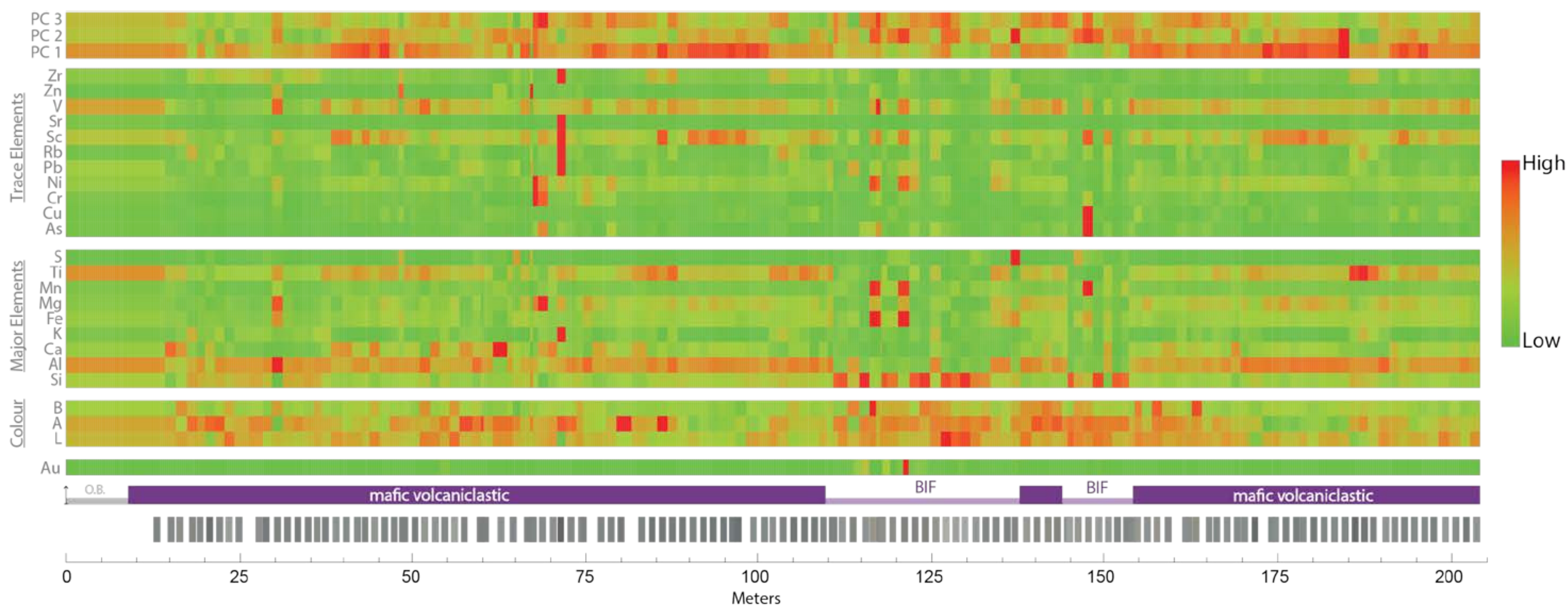

Figure 3 – Heat map showing major and trace element pXRF concentrations rescaled to fall between 0 and 1 (low to high or green to red, respectively) for drill hole M12-1615 (F Zone). Data are plotted alongside a schematic core log that summarizes lithologic variation down-hole. Colour measurements, plotted in true LAB colour space (grey bars), are plotted alongside the schematic borehole log and are also shown numerically within the heat map (LAB). Principle Component scores (PC1, PC2, PC3), described in Lawley et al. (in press), emphasize lithologic variations down-hole and are shown for reference. Note major and minor element concentration and colour changes related to lithologic variation and/or adjacent to Au assay values (provided by Agnico Eagle Mines Ltd.).

Acknowledgements

This work was completed under the auspices of Natural Resource Canada's Targeted Geoscience Initiative (TGI)-4 program. Sally Pehrsson and Vicki McNicoll are thanked for their contribution to fieldwork and regional sampling. The authors would like to thank the cooperation and input from Agnico-Eagle Mines throughout the study period. In particular, Denis Vaillancourt, Robert Fraser, Marjorie Simard and Francine Fallara are thanked for unpublished assays results, borehole logs, and geologic plans/sections for the studied deposits.

References

Aspler, L.B., and Chiarenzelli, J.R., 1996. Stratigraphy, sedimentology and physical volcanology of the Kenik Group, central Ennadai-Rankin greenstone belt, Northwest Territories, Canada: late Archean paleogeography of the Hearne Province and tectonic implications: Precambrian Research, v. 77, p. 59–89.

Bannatyne, M.J., 1958. The geology of the Rankin Inlet area and North Rankin Nickel Mines Limited, Northwest Territories. Unpublished MSc. Thesis, University of Manitoba, Winnipeg.

Carpenter, R.L., 2003. Relative and absolute timing of supracrustal deposition, tectonothermal activity and gold mineralization, West Meliadine region, Rankin Inlet Greenstone Belt, Nunavut, Canada. Unpublished PhD Thesis, University of Western Ontario, 391 p.

Carpenter, R.L., and Duke, N.A., 2004. Geological setting of the West Meliadine Gold Deposits, Western Churchill Province, Nunavut, Canada. Exploration and Mining Geology, v. 13, p. 49−65.

Carpenter, R.L., Duke, N.A., Sandeman, H.S., and Stern, R., 2005. Relative and absolute timing of gold mineralization along the Meliadine Trend, Nunavut, Canada: Evidence for Paleoproterozoic gold hosted in an Archean greenstone belt. Economic Geology, v. 100, p. 567−576.

Knight, R.D., Kjarsgaard, B.A., Plourde, A.P., and Moroz, M., 2013. Portable XRF spectrometry of reference materials with respect to precision, accuracy instrument drift, dwell time optimization, and calibration. Geological Survey of Canada, Open File 7358, 45 p.

Lawley, C.J.M., Dubé, B., Mercier-Langevin, P., Kjarsgaard, B., Knight, R., Vaillancourt, D., in press, Defining hydrothermal footprints at the BIF-hosted Meliadine Gold District, Nunavut, Canada. Journal of Geochemical Exploration.

Miller, A.R., Balog, M.J., and Tella, S., 1995. Oxide iron-formation-hosted lode gold, Meliadine Trend, Rankin Inlet Group, Churchill Province, Northwest Territories. Geological Survey of Canada, Current Research 1995-C, p. 163–173.

Tella, S., Roddick, J.C., and van Breemen, O., 1996. U-Pb zircon age for a volcanic suite in the Rankin Inlet Group, Rankin Inlet map area, District of Keewatin, Northwest Territories. Geologic Survey of Canada, Radiogenic Age and Isotopic Studies Report 9, p. 11–15.

Appendices

Microsoft Excel Worksheet: of_7711_Table_1
Microsoft Excel Worksheet: of_7711_Table_2